ELSEVIER

Journal of Photochemistry and Photobiology A: Chemistry 148 (2002) 183–189

Journal of Photochemistry and Photobiology A:Chemistry

www.elsevier.com/locate/jphotochem

Pathways of phenol and benzene photooxidation using TiO_2 supported on a zeolite

Jian Chen, Lela Eberlein, Cooper H. Langford*

Department of Chemistry, University of Calgary, 2500 University Drive NW, Calgary, Alta., Canada T2N 1N4

Received 24 July 2001; received in revised form 24 October 2001; accepted 24 October 2001

Abstract

The use of photocatalysts supported on adsorbents is gaining substantial attention. Photooxidation of phenol and benzene initiated by light absorption by TiO_2 supported on ZSM-5 zeolite is reported to learn in what ways loading TiO_2 on an adsorbent high silica zeolite modifies the reactions pathways. At equal TiO_2 loading, rates of phenol loss were similar to reactions on P25. In acid media, the major primary products were the result of expected *o*-, *p*-hydroxylation. Catechol and hydroquinone were formed and consumed at comparable rate so that a near steady state persisted for about 400 min. In contrast, secondary reactions were faster on P25 and catechol and hydroquinone concentrations decline systematically from 60 min onward. Beyond trihydroxy species, ring opening became important. The open chain oxygenated species built up little and appear to undergo further oxidation rapidly. The zeolite supported photocatalyst had a maximum efficiency at pH = 3.4 and lost reactivity at higher pH. In basic media, hydroquinone becomes the dominant primary product. Catechol yields decline, but phloroglucinol, undetected in acid, is found. There is evidence of some polymerization with TiO_2 on the adsorbent zeolite support in base that interferes with mineralization. Reactions of benzene may not be simply limited to initial formation of phenol. The are some differences in the pathway for benzene that suggest other initial steps. It is reasonable to infer that there are differences between phenol and benzene adsorption on the catalyst and that benzene can react with species other than an adsorbed OH radical in an alternate the initial step.

Keywords: Supported photocatalyst; Zeolite; Phenol oxidation

1. Introduction

Extensive research has examined the ability of semiconducting materials to promote the degradation and complete mineralization of various pollutants [1–10]. Most of the work has exploited titanium dioxide (TiO_2), a semiconductor that successfully lends itself to this application. TiO_2 has a band gap of ∼3.2 eV which corresponds to photon absorption in the near-UV region, ∼390 nm [11]. Electron–hole pairs generated by radiation may be trapped at the particle surface in aqueous solution where they can act as strong redox agents which can catalyze O_2 oxidation of organic chemicals. Other beneficial characteristics of TiO_2 include the powder being chemically and mechanically robust, resistant to both thermal and photochemical degradation and inexpensive.

Since reactions predominantly occur on the surface, support of TiO_2 on good adsorbents for organic substrates is drawing attention with three potential advantages in mind [3]. (1) The concentration of substrates near the TiO_2 particle is enhanced and the concentration increase may increase rates. (2) Intermediates may be adsorbed and retained. (3) Common adsorbents have long life and may recycle as substrates are mineralized. Zeolite supported TiO_2 has been employed as a catalyst in photoreactions that have previously been performed on bulk powdered P25 TiO_2 alone [3,4,9,12,13]. High silica zeolites can be adsorbents for organics comparable to activated carbon (and zeolite structures offer a range of adsorbent properties). The present study focuses on the photocatalytic degradation of phenol and benzene. A key question concerning zeolite supported TiO_2 photocatalysts is whether the reaction pathways are altered by adsorption on the zeolite. Little information on this point has appeared.

This study reports phenol and benzene pathways on a high silica zeolite supported TiO_2. The influence of the pH on the reaction is also documented. The catalyst chosen [13] for the study is one of the most interesting of a large number that have been prepared in this laboratory. It was reported to be superior to P25 in some circumstances [13] and the surface TiO_2 was characterized by powder X-ray, Raman, and BET measurements. X-ray and Raman are consistent with an anatase structure with some shift of Raman bands at low coverage. The TiO_2 reduces the surface area of the

* Corresponding author. Tel.: +1-403-220-3228; fax: +1-403-289-9488.
E-mail address: chlangfo@ucalgary.ca (C.H. Langford).

1010-6030/02/$ – see front matter
PII: S1010-6030(02)00041-2

zeolite slightly and has little effect on adsorption. Maximum activity was already achieved at low (3–5%) TiO_2 loading. A subsequent paper [14] identified the fraction of the silicate surface covered by TiO_2 by means of ^{1}H-Si CP-MAS NMR and energy filtered TEM location of Ti. At 5% loading, the TiO_2 forms a film of thickness of one unit cell of anatase.

2. Experimental section

2.1. Chemicals

Titanium(IV) tetraisopropoxide (97%) was purchased from Aldrich. P25 titanium oxide was a gift from the Degussa. The ZSM-5 zeolites (ammonium form, $SiO_2/Al_2O_3 = 50$ and 280) and silicalite were purchased from Zeolyst International. Phenol (99%), benzene (99%), catechol (CC) (99%), hydroquinone (HQ) (99%), resorcinol (99%), hydroxyhydroquinone (HHQ) (99%), pyrogallol (PG) (99%), phloroglucinol (PHG) (99%), muconic acid (MUC) (98%) and maleic acid (MLC) (98%) were purchased from Aldrich. HPLC grade acetonitrile (99.99%) and acetic acid (98%) used as solvents in the HPLC mobile phase were purchased from Aldrich. Doubly distilled water was used throughout this work.

2.2. Preparation of the supported titanium oxide catalyst

The TiO_2 sol was synthesized by acid-catalyzed sol–gel formation. The reactant composition consisted of 200 ml of water, 1 ml of nitric acid, and 28.1 g of titanium(IV) tetraisopropoxide dissolved in 10 ml of ethanol. The resulting slurry was peptized for 8 h.

The composite photocatalyst was prepared by thermally binding TiO_2 onto the surface of the ZSM-5 [13]. ZSM-5, saturated with water for 30 min was mixed with TiO_2 sol by stirring for 1 h. Then, this mixture was dried by evaporation at 50 °C for 2–3 h. This was followed by heating at 120 °C overnight and finally the solid was calcined at 450 °C for 11–12 h.

By this procedure, a sample of 3 wt.% of titanium oxide on ZSM-5 was prepared (UC211). It was confirmed earlier [13] that the measured content of TiO_2 in the sample may be calculated from synthetic conditions, as expected. Commercial P25 Degussa powder was used for comparison purposes.

Individual stock solutions of phenol and benzene were prepared in distilled water.

2.3. Photocatalytic experiments

All experiments were performed in a photoreactor shown in Fig. 1. The total reactor volume of this apparatus was 508 ml consisting of a 235 ml Pyrex glass photoreactor with a 288 ml Pyrex reactor reservoir and a cooling jacket. The

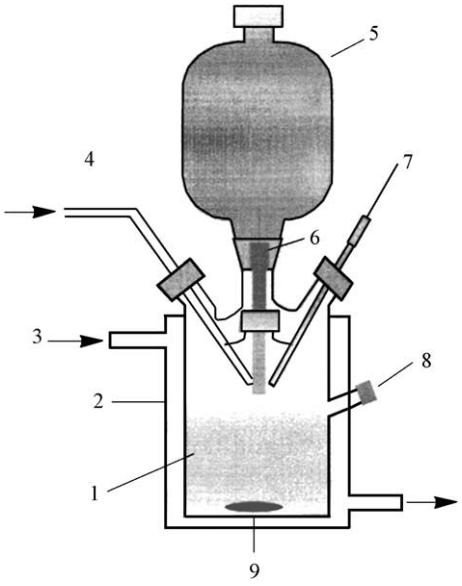

Fig. 1. Photocatalytic reactor: (1) reaction slurry; (2) Pyrex reservoir; (3) cooling water thimble; (4) oxygen sparging tube; (5) gas reservoir; (6) pH meter; (7) thermometer; (8) sample port; (9) stir bar.

irradiation source was a 200 W xenon arc lamp at 181 W output with a 300 nm cut off filter.

Prior to commencing an experiment, 100 ml of phenol or benzene solution at a typical concentration near 100 ppm would be purged with oxygen for 10–15 min before sealing and subsequently purged throughout the course of the experiment. A sample of 500 mg of zeolite photocatalyst (contains 3% TiO_2) or, in the case of P25 TiO_2 only, 15 mg of TiO_2 powder. The mixture was maintained at a temperature of 15 ± 2 °C and stirred constantly and vigorously. The mixture was equilibrated for 30 min to allow for adsorption of the substrate onto the photocatalyst. Total irradiation time was 9 h for each run, unless otherwise stated. Initial substrate oxidation (phenol or benzene) is taken as the reference measure of photocatalytic activity. Periodically, 2 ml of sample was withdrawn from the sample port and filtered through a Millipore filter membrane (0.45 μm pore size, adsorption by such a filter was found to be less than 3%).

2.4. Analysis

Chemical analysis of the filtrate was done using a Waters 486 HPLC with a Supelco reverse phase column of RP-Amide C16 measuring 25 mm × 4.6 mm. The solvent consisted of a mixture of water (85%) with acetic acid (2.4%) and acetonitrile (15%) at a flow rate of 0.5 ml min^{-1}. HPLC/MS runs were conducted by the Food Analysis Laboratory of Agriculture Canada in Calgary.

2.5. Phenol adsorption in the dark

The adsorption capacity of the zeolite supported titania photocatalyst for phenol substrate was evaluated in

aqueous media. A 200 ml sample of aqueous phenol solution (90 ppm) was mixed with 1 g of the catalyst. The suspension was shaken at $13 \pm 2\,^{\circ}C$ and the phenol concentration in solution was measured in the dark over an 18 h time period. The results indicate that 15–20% of phenol can be adsorbed from the solution onto the photocatalyst surface, reaching >90% of equilibrium in 30 min. The 18 h run also demonstrates that the degradation of phenol is a photoprocess as no continuous removal of phenol occurs as it does with irradiated catalytic samples.

3. Results

3.1. Phenol reaction kinetics

A comparison of the activity of the supported catalyst and P25 TiO_2 was conducted. The disappearance of the substrate from the reaction mixture was monitored as a function of time of irradiation with a xenon lamp at an intensity of 4.2×10^{-5} einstein min^{-1}. Fig. 2 shows the plots of the observed phenol concentration changes as a function of time at pH = 3.4.

The loss of substrate was fitted to the logarithmic expression for first-order kinetics:

$$\log[C]_t = -kt + \log[C]_0$$

where $[C]_0$ and $[C]_t$ represent the concentration (ppm) of the substrate in solution at time zero and time t of illumination, respectively, and k represents the apparent rate constant (min^{-1}). The inset diagram is a plot of the data in the main diagram to show the rate law. For both reaction mixtures, plots of $\log C$ as a function of time yield straight lines fitting first-order kinetics with respect to the substrate which is, at least, a good approximation. We will see below that overall kinetics are complex since secondary photolysis (oxidation of intermediates) becomes important in the course of the reaction. With an initial phenol concentration of 94 ppm the first-order reaction rate constant was $k = 1.1 \times 10^{-2}\,s^{-1}$ for the supported catalyst reaction and $k = 1.7 \times 10^{-2}\,s^{-1}$ for the equivalent loading P25 TiO_2 reaction. Clearly, the supported catalyst has similar photocatalytic activity to P25 TiO_2 although it was deposited on the zeolite surface with less dispersion than the P25 TiO_2 in solution. The good reactivity at low titania loading implies favorable light collection with little loss due to supports and relatively efficient access by zeolite adsorbent substrates to photoactive sites.

3.2. Phenol intermediate products and reaction pathway

In a photocatalytic process the primary step is, of course, the photogeneration of pairs of electrons and holes, which must be trapped to avoid recombination. It is widely accepted that the surface hydroxyl groups are the likely traps for holes [15]:

$$OH^- + h^+ \rightarrow OH^{\bullet}\,(surf)$$

Traps for electrons are adsorbed oxygen species according to the following equations:

$$O_{2(g)} \rightarrow O_{2(ads)}, \qquad O_{2(ads)} + e^- \rightarrow {O_{2(ads)}}^-$$

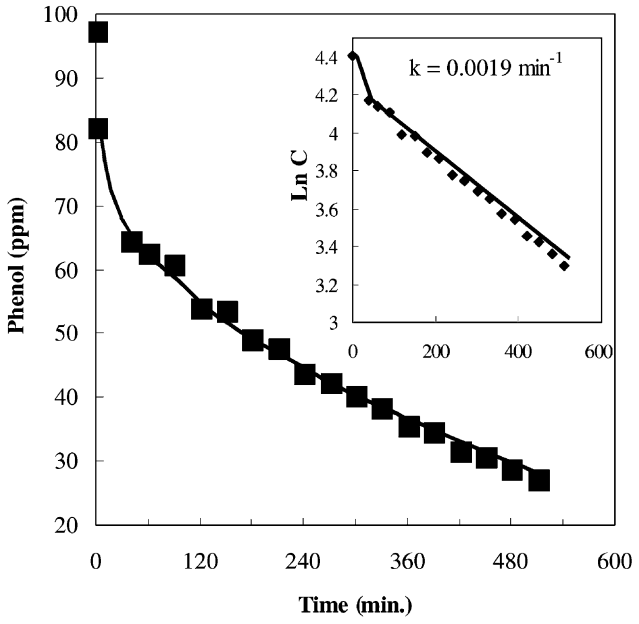

Fig. 2. Photocatalytic oxidation of phenol in the presence of supported catalyst: 94 ppm (1 mM) of phenol, 1 g supported catalyst, 200 ml solution, initial pH 3.5, 300 nm cut off.

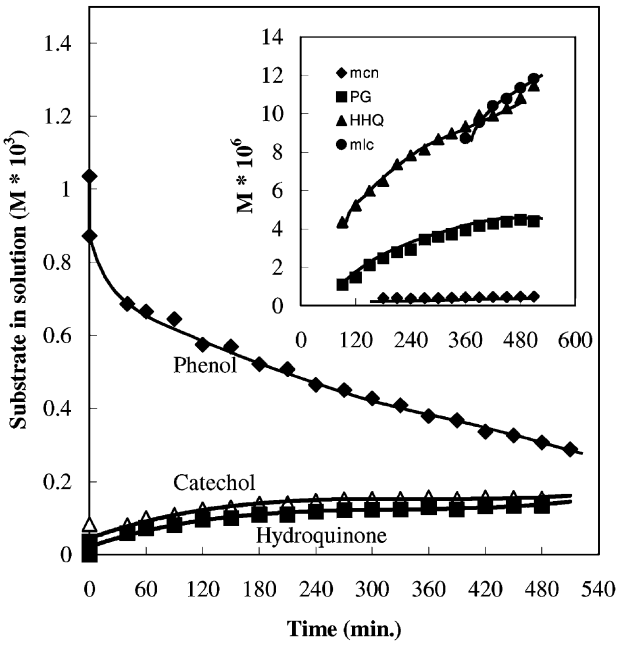

Fig. 3. Characterization of the intermediates produced in the photocatalytic oxidation of phenol in the presence of supported catalyst in acidic medium.

The superoxide species is unstable and reactive. It may evolve in several ways

$$O_{2(ads)}{}^{-} + H_2O \rightarrow OH^{-} + HO_2{}^{\bullet},$$

$$2HO_2{}^{\bullet} \rightarrow H_2O_2 + O_2$$

Thus as a consequence of the primary steps of electron and hole trapping, several species are produced which can be involved in the reaction [11,15–18]. TiO_2 photocatalyzed degradation of phenol proceeds through the stepwise formation of intermediates. The pathway of phenol photooxidation using TiO_2 in acidic medium has been reported [19–21], but never using a zeolite supported catalyst. Here, we focus on the comparison of the supported catalyst with P25 TiO_2, and consequently the effect of having an adsorbing support on the mechanistic pathway of phenol degradation.

HPLC analysis of the solution from phenol degradation experiments revealed the presence of several intermediate species. The components CC and HQ were detected as the major aromatic intermediate species present. Time evolution of the intermediates for both zeolite supported and P25 TiO_2 phenol oxidations in acidic medium are displayed in Figs. 3 and 4, respectively. On the supported catalyst, the total amount of CC and HQ present accounts for up to 70% of the phenol degraded and remains near this value (a near steady state) up to nearly 400 min (Fig. 5). This implies that secondary oxidation of CC and HQ is occurring at about the same rate that they are formed from phenol. In contrast, on P25 TiO_2 the intermediates reach a peak within 1 h, after which they decline steadily in concentration. This suggests faster secondary (compared to primary) photolysis on P25 TiO_2. Additional intermediate species detected include HHQ, PG, MLC and MUC found at 10^{-1}–10^{-3} of the concentration of CC and HQ. HHQ is formed as the major secondary product via either CC and/or HQ. It is produced in greater concentrations on P25 TiO_2 than on the supported catalyst reaction, confirming faster secondary photolysis. PG can be formed from CC. It is found in comparable concentrations on both catalysts.

MUC and MLC involve ring opening, which occurs from the degradation of the earlier intermediates. With the supported catalyst, MLC appears after 360 min of irradiation reaching a concentration of $\sim 12 \times 10^{-6}$ M with indication of further increase. In comparison, on the P25 TiO_2, MLC is detected earlier (240 min) but only reaches a maximum of $\sim 6 \times 10^{-6}$ M, then declines. This is an interesting observation as it suggests that the supported catalyst can promote ring opening, an important feature in degradation reactions. However, it may also emphasize faster secondary photolysis on P25 TiO_2. Several other small peaks were detected but were not identified largely due to their low concentrations. These peaks tended to have short retention times occurring later on in the reaction and were attributed to very polar products such as the aldehydes and carboxylic acids, that lead to eventual mineralization.

The following scheme summarizes the possible degradation pathway for phenol in acidic medium: the close parallel between HQ and CC reminds us that they may be interconverted:

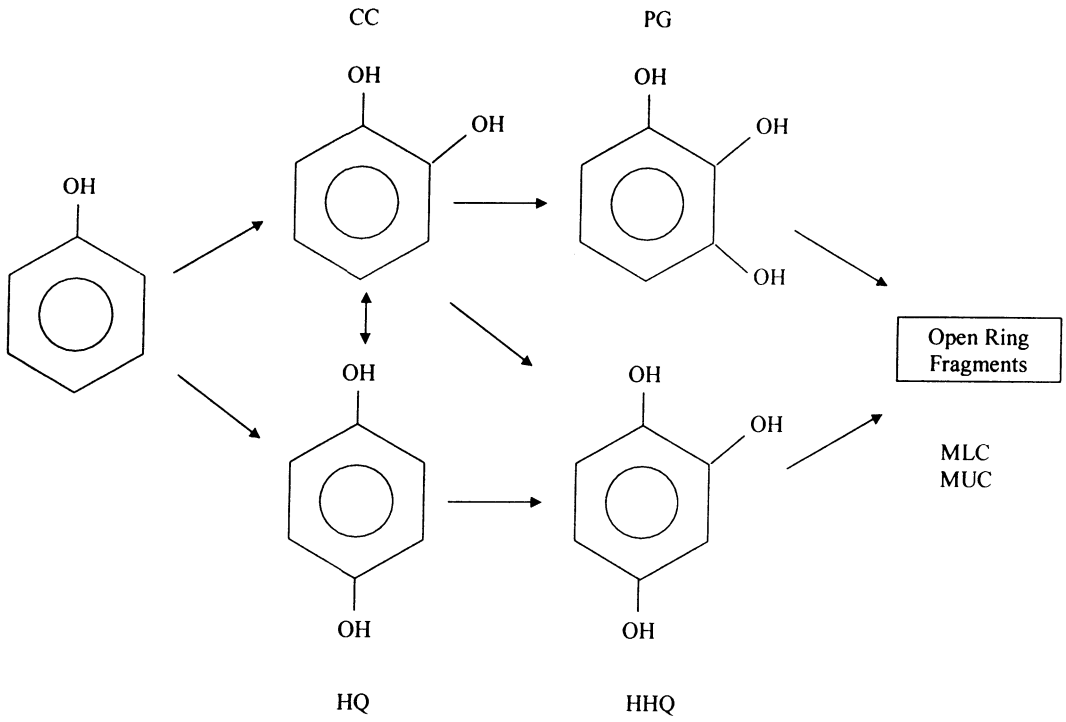

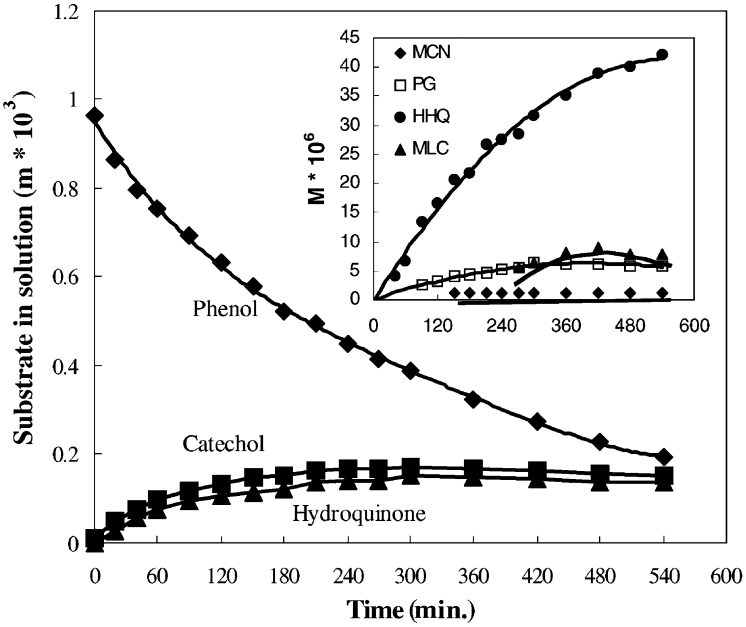

Fig. 4. Characterization of the intermediates produced in the photocatalytic oxidation of phenol in the presence of P25 TiO_2 in acidic medium.

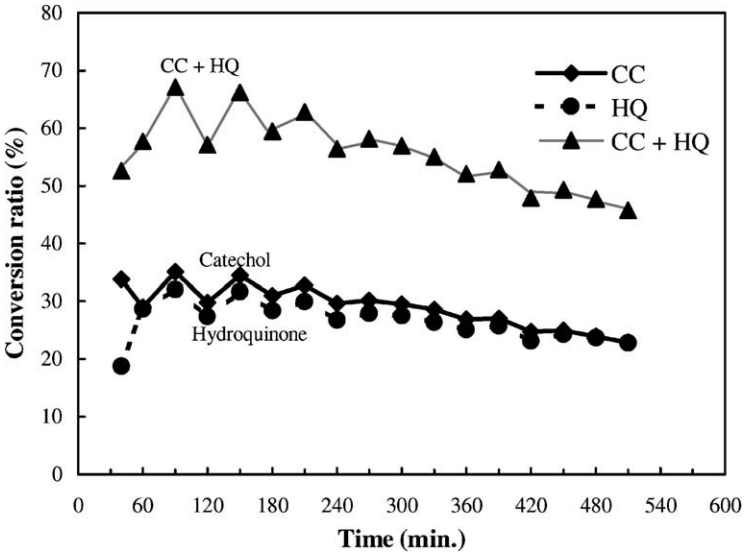

Fig. 5. Conversion ratio of phenol photocatalytic oxidation to CC and HQ on supported catalyst in acidic medium.

3.3. Influence of pH

The influence of pH on photocatalytic degradation of phenol was monitored with respect to both the rate constants and the intermediate products. Fig. 6 displays kinetics at pH 10.9. For the reactions involving the supported catalyst, pH 3.4 is the optimum for the decomposition of phenol. There is a clear trend showing that the oxidative process becomes less efficient at higher pH levels.

In an acidic medium, catalyst mediated phenol degradation gave CC and HQ as the major intermediates with CC appearing in the highest concentration. In a basic medium, HQ is the predominant intermediate with HHQ, PHG, and MCN as the secondary intermediates. A different intermediate, PHG, not detected in acidic medium is found here. Formation of PHG occurs via hydroxylation of resorcinol thus supporting *meta* attack of the substrate. The decrease in CC production with increasing solution pH (by pH 11, CC disappears completely from solution with only HQ being produced) is a known feature of TiO_2 photolysis and may result from thermal as well as photolytic chemistry.

A significant (and negative) feature of the supported catalyst in base in appearance of a pink/brown color in the reaction solution that poisons the catalyst surface. HPLC–MS

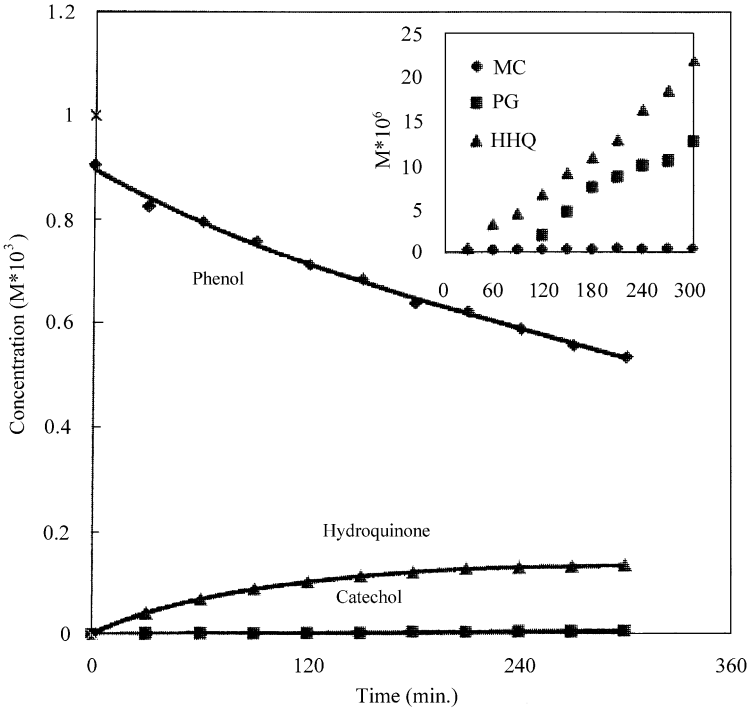

Fig. 6. Characterization of intermediates produced in the photocatalytic oxidation of phenol in the presence of supported TiO_2 in basic medium.

identifies compounds in the *m*/*e* range from 180 to 400, suggesting two to four ring units. Dimerization and oligomers of phenols may arise from the relatively long lifetime of the intermediate *p*-hydroxybenzyl radical produced at high pH conditions. A further feature of the supported catalyst is the formation of small amounts of a white film that does not adhere to catalyst particles. Separation and MS analysis indicate a polymer with MW up to 1580.

On P25 TiO2, degradation of phenol at pH 12 also gives HQ as the predominant intermediate with CC, RES, HHQ, PHG and PG as the secondary intermediates. These results agree with earlier reports [22]. HQ is rapidly produced at relatively high concentrations and then falls steadily throughout the course of the reaction to an almost negligible value. This is probably due to the occurrence of faster secondary reactions. Unlike behavior on the supported catalyst, the two types of polymer formations are *not* observed.

3.4. Benzene photodegradation

Adsorption of benzene by ZSM-5 zeolite was about twice the phenol adsorption. The degradation of benzene was also fitted to first-order kinetics. The rate constants were $5.3 \times 10^{-5}\,s^{-1}$ (pH = 10.9) and $5.7 \times 10^{-5}\,s^{-1}$ (pH = 3.5) on the zeolite supported catalyst and $9.3 \times 10^{-5}\,s^{-1}$ (pH = 10.9) on P25. The main primary intermediate was phenol and its concentration increases throughout the run. For the basic solution run, in 300 min, about 70 ppm of benzene had been photo-degraded but only about 15 ppm of phenol was found (benzene was not lost in dark blanks). PGL was a more important species than HQ. Oxidation of benzene on P25 TiO_2 yielded measurable MUC at 60 min, much earlier than in phenol oxidations. These observations suggest that the benzene pathway is not simply the phenol pathway with an initial step of hydroxylation of benzene. It seems likely that benzene undergoes an initial oxidation including products more oxidized than phenol. This can reflect either oxidation via direct hole attack on benzene or attack by radicals derived from O_2.

4. Summary remarks

In summary, we can observe that supporting TiO_2 on a zeolite does not deliver all of the anticipated advantages. The supported photocatalyst and P25 TiO_2 exhibit similar reactivity and pathway. However, we see that the supported catalyst can introduce new problems as illustrated by polymer formation in basic media. One of the possible advantages of zeolite supports might arise from the production of H_2O_2 at the photocatalyst and the known capacity of zeolites to catalyze peroxide oxidations. So far, little if any evidence for such contributions has emerged despite a careful search. The suggestion that intermediates will be better retained on a strongly adsorbing support overlooks the possibility that specific adsorption on TiO_2 may be critical to further reaction. The relatively slower contribution of secondary reaction of CC and HQ on zeolite supported TiO_2

may reflect the competition between the zeolite surface and chelation of the dihydroxy species to titanium Lewis acid sites.

Acknowledgements

We thank the Natural Sciences and Engineering Research Council of Canada and Trojan Technologies of London, Ont., for support of this work.

References

[1] D.F. Ollis, H. Al-Ekabi (Eds.), Photocatalytic Purification and Treatment of Water and Air, Elsevier, Amsterdam, 1993.
[2] N. Serpone, E. Pelizzetti (Eds.), Photocatalysis—Fundamentals and Applications, Wiley/Interscience, New York, 1989.
[3] H. Yoneyama, T. Torimoto, Catal. Today 58 (2000) 133.
[4] K.J. Green, R. Rudham, J. Chem. Soc., Faraday Trans. 89 (1993) 1867.
[5] J. Cunningham, G. Al-Sayyed, S. Srijarani, in: G.R. Helz, R.G. Zepp, D.G. Crosby (Eds.), Aquatic and Surface Photochemistry, Lewis Publishers, Boca Raton, FL, 1994 (Chapter 22).
[6] M. Aldullah, G.C. Low, R.W. Mattews, J. Phys. Chem. 94 (1990) 6820.
[7] R.W. Mattews, Water Res. 24 (1990) 653.
[8] R.W. Mattews, J. Catal. 113 (1998) 549.
[9] X. Liu, K.K. Iu, J.K. Thomas, J. Chem. Soc., Faraday Trans. 89 (1993) 1816.
[10] J. Sabate, M.A. Anderson, M.A. Aguado, S. Gimenez, S. Cervera-March, C.G. Hill Jr., J. Mol. Catal. 71 (1992) 57.
[11] M.R. Hoffman, S.T. Martin, W. Choi, D.W. Bahnemann, Chem. Rev. 95 (1995) 69.
[12] T. Torimoto, S. Ito, S. Kuwabata, H. Yoneyama, Environ. Sci. Technol. 30 (1996) 1275.
[13] Y. Xu, C.H. Langford, J. Phys. Chem. 99 (1995) 11501.
[14] E. Vaisman, R.L. Cook, C.H. Langford, J. Phys. Chem. B 104 (2000) 8679.
[15] N. Serpone, J. Photochem. Photobiol. A 104 (1997) 1.
[16] G.P. Lepore, B.C. Pant, C.H. Langford, Can. J. Chem. 71 (1993) 2051.
[17] C. Arbour, D.K. Sharma, C.H. Langford, J. Phys. Chem. 94 (1990) 331.
[18] P.V. Kamat, N.M. Dimitrijevic, Sol. Energy 44 (1990) 83.
[19] K. Okamoto, Y. Yamamoto, H. Tanaka, M. Tanaka, A. Itaya, Bull. Chem. Soc. Jpn. 58 (1985) 2015.
[20] V. Augugliaro, L. Palmisano, A. Sclafani, C. Minero, E. Pelizzetti, Toxicological and Environmental Chemistry, Vol. 16, Science, GB, 1988, pp. 89–109.
[21] C.S. Turchi, D.F. Ollis, J. Catal. 119 (1989) 483.
[22] A. Sclafani, L. Palmisano, M. Schiavello, in: G.R. Helz, R.G. Zepp, D.G. Crosby, Aquatic and Surface Photochemistry, Lewis Publishers, Boca Raton, FL, 1994, p. 419.